frontiers | Frontiers in Physics

TYPE Review
PUBLISHED 14 September 2022
DOI 10.3389/fphy.2022.995361

OPEN ACCESS

EDITED BY
Jingbiao Chen,
Peking University, China

REVIEWED BY
Yang Shiyu,
Lanzhou Instute of Physics, China
Xiumei Wang,
PKU-HKUST Shenzhen-Hong Kong Institution, China

*CORRESPONDENCE
Jiayu Dai,
daijy@shao.ac.cn

SPECIALTY SECTION
This article was submitted to Atomic and Molecular Physics, a section of the journal Frontiers in Physics

RECEIVED 15 July 2022
ACCEPTED 29 July 2022
PUBLISHED 14 September 2022

CITATION
Dai J, Liu T, Cai Y, Chen Z and Li Q (2022), Review of the development of the hydrogen maser technique and a brief introduction to its space applications.
Front. Phys. 10:995361.
doi: 10.3389/fphy.2022.995361

Review of the development of the hydrogen maser technique and a brief introduction to its space applications

Jiayu Dai[1]*, Tiexin Liu[1], Yong Cai[1], Zhichun Chen[1] , Qi Li[1,2]

[1]Laboratory of Time & Frequency Technology Research, Shanghai Astronomical Observatory, Chinese Academy of Sciences, Shanghai, China, [2]School of Materials Science and Engineering, Shanghai University, Shanghai, China

Since 1960, when the first hydrogen frequency standard, the microwave amplification by stimulated emission of radiation (maser), was developed in the laboratory of Norman Ramsey at Harvard University, the performance of its frequency stability and technique development have been closely related to scientific research. A variety of H-maser designs have been developed for the demands of space science applications, including the deep space network (DSN) and the gravity probe (GP) experiment. H-maser is one of three well-developed microwave atomic frequency standards and is widely used worldwide in both ground and on-board-based settings. Along with upgrades to the frequency stability performance of the H-maser, improved knowledge of the world has also been reported.

KEYWORDS

hydrogen maser, time and frequency standard, atomic frequency standard, space science applications, astronomy

1 Introduction

The hydrogen microwave amplification by stimulated emission of radiation (H-maser) is an atomic frequency standard widely used in ground and on-board-based settings. Rather than focusing only on comparing the H-maser to the other two well-developed atomic frequency standards; namely, the cesium beam atomic frequency and rubidium frequency standards, this review discusses the frequency accuracy and stability performance, the volume and mass weight for particular applications, and the power consumption of the H-maser. We also review some of its fields of application.

The H-maser is larger in volume than the other two frequency standards. The frequency accuracy of the H-maser is approximately 1×10^{-12} [1], which is not sufficient for a primary frequency standard compared to the 1×10^{-13} accuracy of the Cesium beam standard. The stability of the frequency output of the H-maser is typically a few parts in 10^{15} for an average time interval, τ, of the order of 10^{3}–10^{5} s. The accuracy and stability performance of the H-maser are mainly limited by factors such as the relaxation time, thermal noise, wall shift, second-order Doppler shift, and second order Zeeman effect, depending on the particular design. Comparisons of the frequency stability performance

TABLE 1 Stability performance of the MHM-2020 active H-maser.

Average time, τ	ADVE
1 s	$\leq 1.5 \times 10^{-13}$
10 s	$\leq 2 \times 10^{-14}$
100 s	$\leq 5 \times 10^{-15}$
1,000 s	$\leq 2 \times 10^{-15}$
10,000 s	$\leq 1.5 \times 10^{-15}$

TABLE 2 Stability performance of the 5071A cesium clock primary frequency standard.

Average time, τ	ADVE
0.01 s	$\leq 7.5 \times 10^{-11}$
0.1 s	$\leq 1.2 \times 10^{-11}$
1 s	$\leq 5.0 \times 10^{-12}$
10 s	$\leq 3.5 \times 10^{-12}$
100 s	$\leq 8.5 \times 10^{-13}$
1,000 s	$\leq 2.7 \times 10^{-13}$
10,000 s	$\leq 8.5 \times 10^{-14}$
100,000 s	$\leq 2.7 \times 10^{-14}$
5 days	$\leq 1.0 \times 10^{-14}$
30 days	$\leq 1.0 \times 10^{-14}$

TABLE 3 Stability performance of the FS725—benchtop rubidium frequency standard.

Average time, τ (s)	AVAR
1	$< 2 \times 10^{-11}$
10	$< 1 \times 10^{-11}$
100	$< 2 \times 10^{-12}$

of the H-maser to those of the Cesium beam tube and Rubidium frequency standards are reported in Refs. [2–4]. Tables 1–3 demonstrate the best performance of the H-maser for a τ value of approximately 10^3.

The H-maser dates back to the 1960s [1] or even earlier. The H-maser experiments originated in an effort to develop a device that proved four features [5]: 1) a narrow resonance line; 2) a reduced broadening of the line due to some effects; 3) a reduced first-order Doppler shift; and 4)a favorable signal-to-noise ratio. H-maser-related studies performed world-wide demonstrated its applications in the fields of time-keeping, the deep space network (DSN), and the very long base line interferometry (VLBI) network for radio astronomy and geophysics, as well as the global navigation satellite system (GNSS) and others. Improvements in the stability performance and reduced mass and volume make the H-maser competitive in modern scientific research applications.

A typical stability performance of 10^{-15} to 10^{-16} per day has been reached for the traditional design and a better than 1×10^{-16} has been demonstrated in the laboratory [6] (Figure 1). The passive H-maser has also reached a one-day average frequency stability of a few parts in 10^{15}.

To help us to understand how the H-maser has been developed and upgraded along with the progress in its scientific applications, Section 2 provides a brief description of the physical principles of the H-maser and pertinent technique developments. Section 3 describes its applications in scientific space experiments and astronomical research. Finally, Section 4 briefly discusses the future of the H-maser.

2 Review of the H-maser

Updates to the H-maser have recently slowed, perhaps for the following reasons.

First, the theory of the H-maser had already been well studied; thus, technique development seems to have reached a ceiling. Even the most recent update of the best stability performance in Russia was mainly contributed by a single-state-selected beam design that had been proposed long before. Secondly, it takes time to develop new theories for improved performance and technology upgrades, including material science research and industry manufacturing. Finally, recent efforts have focused on reducing its volume and mass, as well as improving its robustness for on-board space applications. These may explain why the H-maser is described as a well-developed product.

2.1 Principles and design

Like other frequency sources, the frequency signals of the H-maser occur due to the periodic motion of H atoms. The principles can be roughly summarized as follows: first, the H-maser obeys the theory of conservation of energy, in which the interactions between atoms and electromagnetic waves are expressed by Formula 1. Second, a resonant oscillation leads to the amplification of the useful atomic signal.

$$\Delta E = E_m - E_n = h\nu_{mn} \tag{1}$$

Following these principles, the H-maser is mainly composed of a physical unit, which provides a high-quality reference signal in form of an electromagnetic emission through hyperfine transitions of ground atomic hydrogen, as well as an electrical unit that includes a quartz crystal oscillator that is locked to the physical output to provide the stable frequency signal outputs of

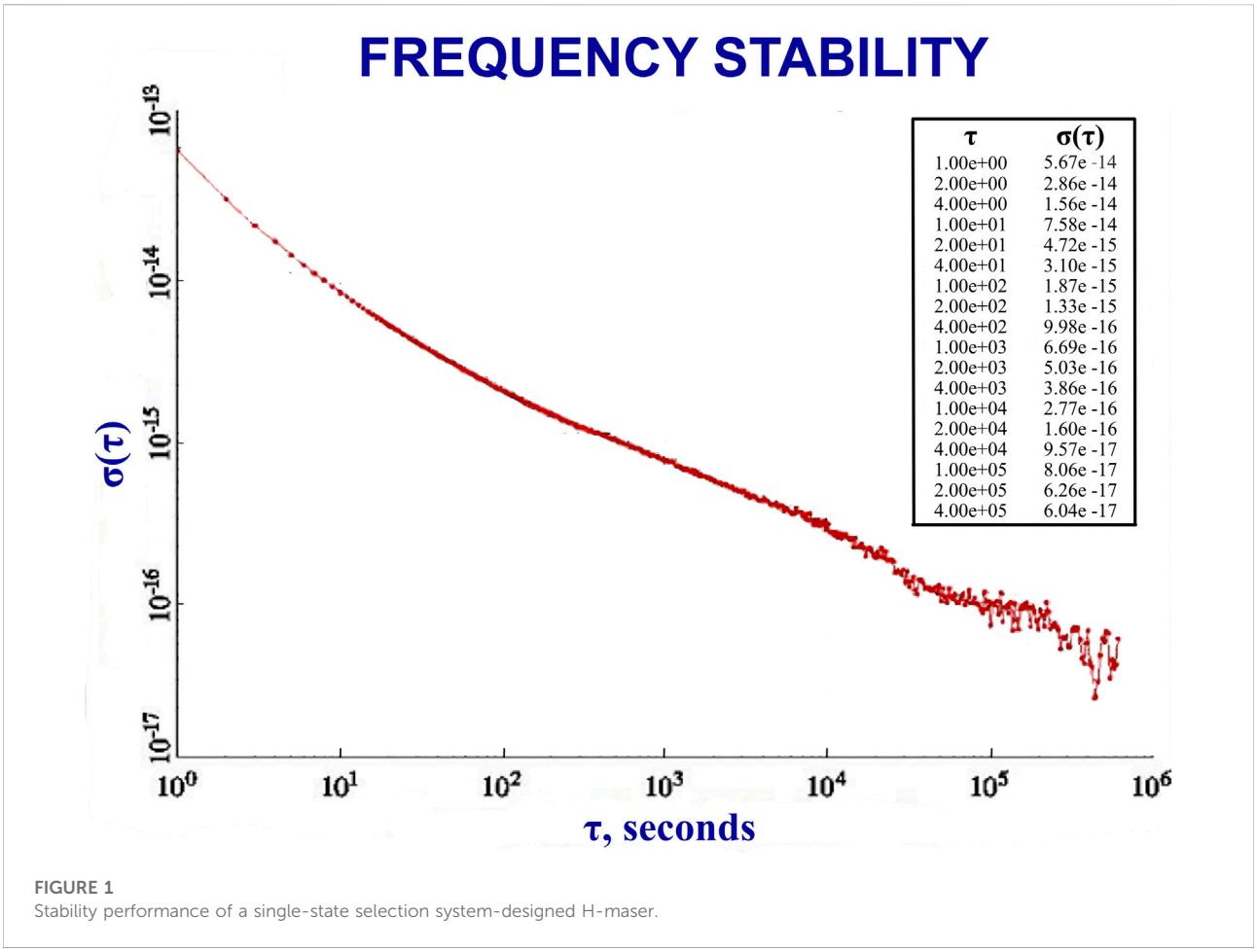

FIGURE 1
Stability performance of a single-state selection system-designed H-maser.

the H-maser, as shown in Figure 2A [7]. The normal optional standard frequency outputs of the H-maser are 5, 10, 20,. . ., 100 MHz, and 1 pps. While any possible transitional radiation can theoretically be used as a reference signal to lock the quartz crystal oscillator in the electrical unit, since the transitional frequencies are sensitive to environmental effects, the reference signal must be the one between two least-sensitive energy levels. For the H-maser a useful transition is that of the ground hydrogen ($n = 1$) from state ($F = 1$, $m_F = 0$) to a lower state ($F = 0$, $m_F = 0$), as shown in Figure 2B [1]. However, although both spontaneous transitions and transitions induced by perturbations can happen in principle in the physical unit, and the corresponding electromagnetic radiation will be emitted, the signal quality of the spontaneous transition is not sufficient for use in the electrical unit. Due to the low number of such transitions, they likely disappear in the background noise of the environment. To make the signal-to-noise ratio high enough for the electrical unit, large numbers of simultaneous transitions are required. Since the transitional signal magnitude is proportional to the population difference of the energy levels, the solution is induced transitions. In other words, by gathering ($F = 1$, $m_F = 0$) atoms in a container and increasing their fractional population, a sufficiently large number of transitions from ($F = 1$, $m_F = 0$) to ($F = 0$, $m_F = 0$) can be simultaneously induced by a stimulating signal, with a corresponding radiation emission of around 1.420405751 GHz.

Furthermore, to provide self-sustained oscillation possible, for example, in an active H-maser, the energy delivered by the atomic transitional radiation should be at least high enough to compensate for the loss of the practical resonant structure design. This requires numerous atoms at the energy level of ($F = 1$, $m_F = 0$) as well as a large population difference between the two levels of ($F = 1$, $m_F = 0$) and ($F = 0$, $m_F = 0$). This can be achieved through so-called population inversion. Secondly, the population difference between the two energy levels should be even larger to output a sufficiently large atomic transitional signal to contribute to the frequency stability performance, as shown in Eqs 2, 3.

More detailed principles of active H-maser systems have been published previously [1, 5, 8, 9]. The time domain frequency stability is given as the Allan Deviation, as shown in Eqs 2, 3.

When, 0.1 s < τ < 10 s:

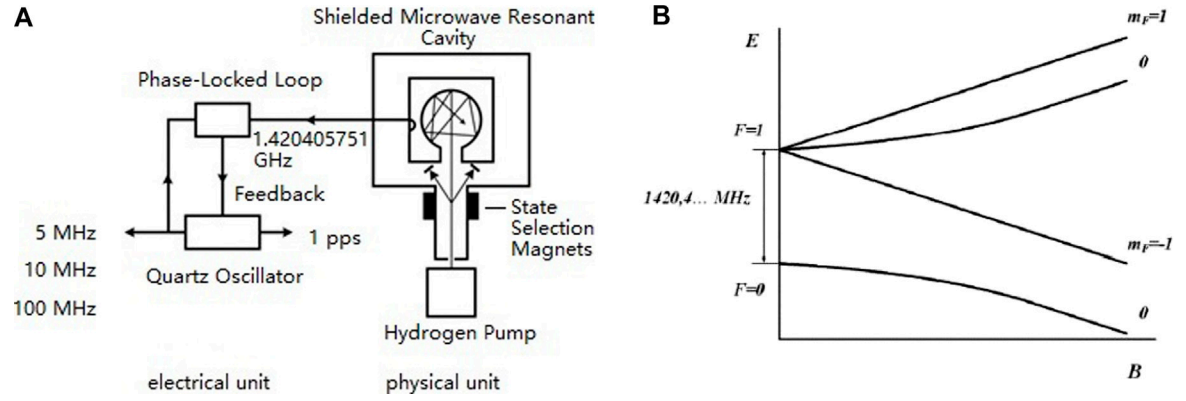

FIGURE 2
(A) Schematic diagram of the standard active H-maser; **(B)** energy requirements for the hyperfine ground S-state hydrogen on the magnetic field.

$$\sigma_y(\tau) = \frac{\beta kT}{\nu_0^2 P_a \tau}\left(1 + F\frac{P_a}{P_r}\right) \tag{2}$$

and when, $\tau > 10$ s:

$$\sigma_y(\tau) = \frac{1}{Q_a\sqrt{\tau}}\sqrt{\frac{kT}{2P_a}} \tag{3}$$

where β is a constant, k is the Boltzmann constant, T is the temperature in Kelvin, P_r is the power received by the input amplifier, F is the amplifier noise factor, P_a is the power delivered by atoms, and $Q_a$is the quality factor of the atomic resonance.

The stability performance of H-maser output mainly depends on the circuit quality for an average time interval of $0.1\text{ s} < \tau < 10$ s. The long-term stability performance is influenced by factors such as the second-order Doppler effect, collisional spin exchange, etc. Therefore, the electrical and physical units play roles in the improvements in H-maser performance.

The flux of hydrogen atoms is also critical based on the relationship between the power, ΔP, radiated by H atoms initially in the state of ($F = 1$, $m_F = 0$) and the atomic hydrogen beam, I, given by Eqs 4, 5 [5, 10]. To provide oscillation in the maser, the effective H atomic beam flux should be greater than the minimum flux, I_{th}, given in Formula 6.

$$\Delta P = \frac{1}{2} Ih\nu \frac{\theta^2}{1 + \theta^2 + \delta^2} \tag{4}$$

$$\theta^2 = \frac{\langle x^2\rangle}{\gamma^2} = \frac{W}{W_c} \tag{5}$$

$$I_{th} = 4\pi\frac{W_c}{Qh} \tag{6}$$

where h is the Planck constant, W is the energy stored in the cavity, and Q is the quality factor of the cavity.

I represents the flux of atoms ($F = 1$, $m_F = 0$). In the evaluation of the fractional population of atoms at this level, the original four hyperfine states are considered to be equally distributed over atoms. This approximation is made only when $e^{(-\Delta E/kT)} \to 1$. For room-temperature H-masers, the energy separations are three orders smaller than the kT when $T = 300$ K. Therefore, for simplicity, $\Delta E/kT \to 0$, although they are not rigorously equally distributed. However, this is not correct for low-temperature H-maser.

The mechanism of passive H-maser is similar to that of active H-maser, except that the physical unit oscillation cannot be self-sustained due to the increased loss when reducing the volume of the microwave resonant cavity. This loss requires compensation by an input from the external electrical circuit to maintain a continuous oscillation. Meanwhile, an extra perturbation is also input. Hence, a sacrifice of the frequency stability is inevitable when reducing the mass and volume of the physical unit for satellite on-board applications. The frequency stability performance [8], also given in form of time domain Allan Deviation, is shown in Formula 7:

$$\sigma_y(\tau) = \frac{A}{Q_a\sqrt{\tau}}\sqrt{\frac{kT}{2P_a}} \tag{7}$$

where A is a constant that depends on the cavity structure.

2.2 Development of H-maser techniques

We focus on reviewing the technique developments only for the physical H-maser units, since the transitional signal contributes to both short and long-term stability. Moreover, the quality of the transitional signal is so sensitive to the environment that the practical physical package must be

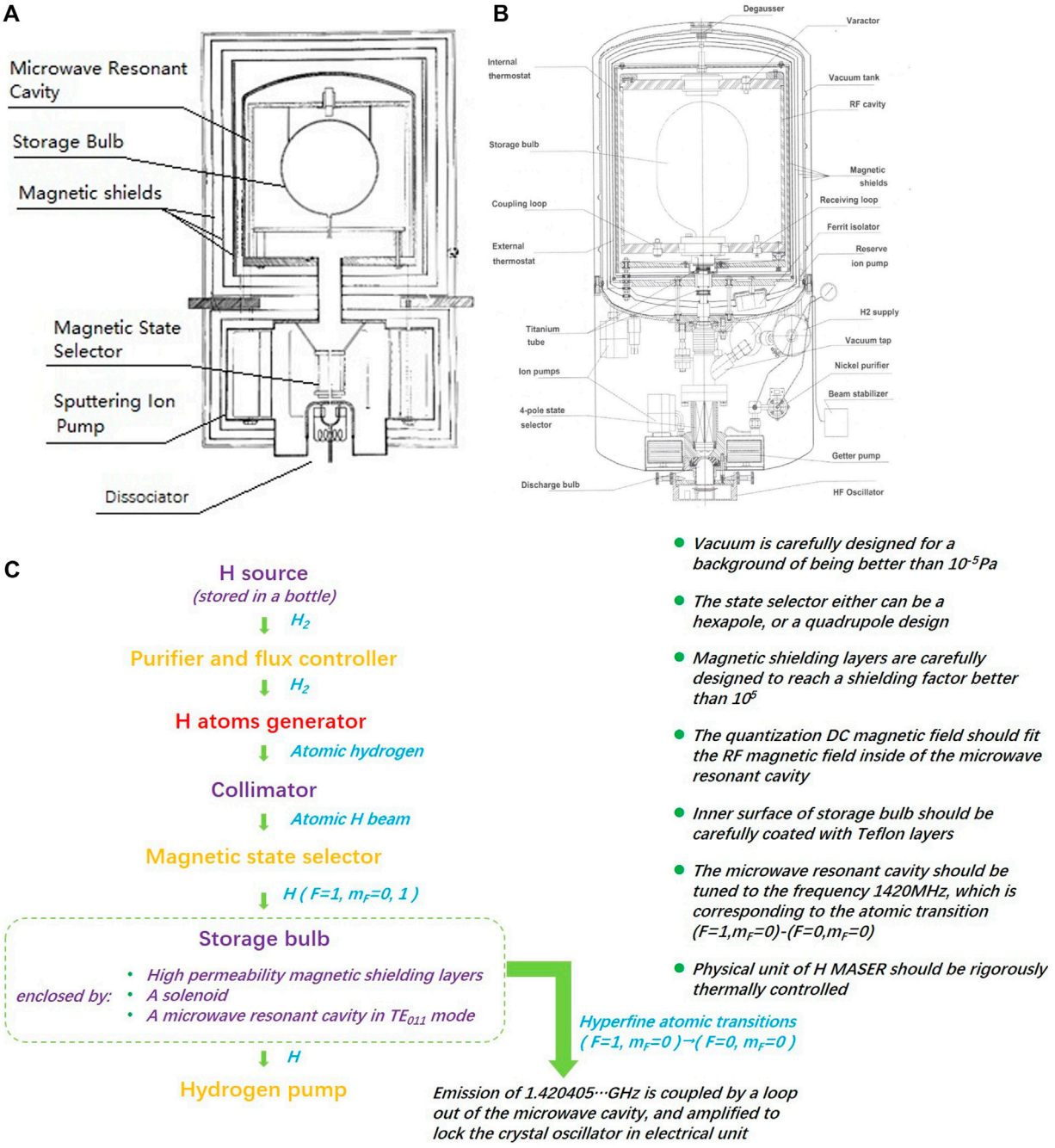

FIGURE 3
Schematic diagram of the standard active H-maser. **(A)** An H-maser unit for a satellite experiment in the 1960s; **(B)** a VCH 1003M unit; **(C)** summary of the standard H-maser unit.

carefully designed to ensure the precision and stability of the maser output frequency. The practical active H-maser of the 1960s and a modern design are shown in Figures 3A,B [11, 12]. The standard active H-maser physical unit design is roughly summarized in Figure 3C.

2.2.1 Hydrogen source

A large amount of pure hydrogen is required to provide a sustained oscillation and ensure a sufficient source of hydrogen for the entire H-maser working period. First, the hydrogen source was designed as a bottle with a high H_2 gas pressure.

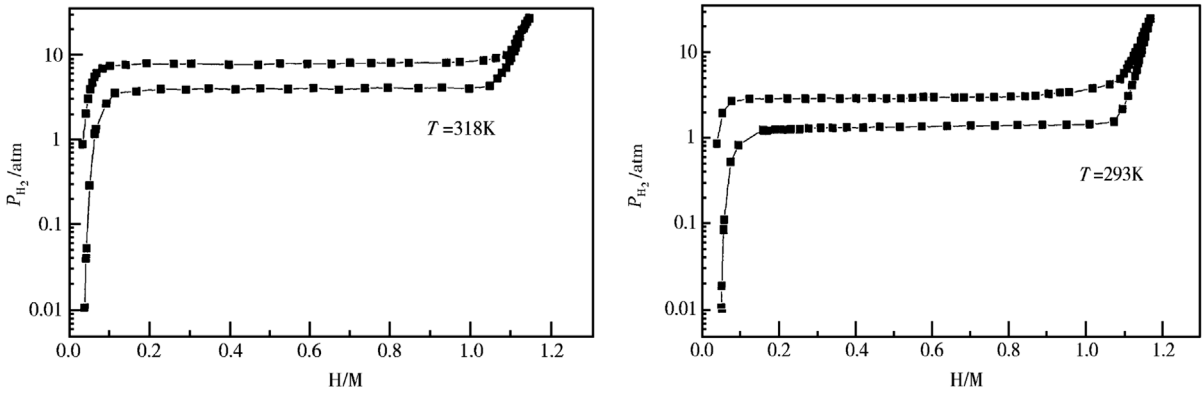

FIGURE 4
Pressure of output of the hydrogen source of a design using a $LaNi_5$ alloy.

However, this was soon replaced by a design that utilized a reversal chemical reaction of H_2 with alloys such as the rare Earth elements, $LaNi_5$ (Formula 8). The replacement extended the working lifetime of the H-maser not only by increasing the storage capacity for the same bottle volume but also by reducing hydrogen leakage. Since hydrogen atoms are small in dimension, they can penetrate through the bottle wall, which is made of steel. The speed of penetration is proportional to the pressure difference. The upgraded design reduced the pressure and, hence, the pressure difference between the two sides of the wall. In addition, by adjusting the components of the alloy compounds, the hydrogen source can output H_2 with an approximately constant pressure (Figure 4 [13]). The output pressure of H_2 can be adjusted by varying the container temperature. Thus, it became easier to regulate the H_2 flux compared to the previous design.

$$\mathrm{LaNi_5} + \mathbf{3H_2} \underset{\text{slightly heated}}{\overset{(2-3)\times10^5\,\mathrm{Pa}}{\rightleftharpoons}} \mathrm{LaNi_5H_6} \qquad (8)$$

The hydrogen then enters a component called the purifier through a connection via a thin stainless-steel tube. The purifier was once made from an alloy pellet comprising 70% palladium and 30% silver [10] and acted to provide and control the flux of purified hydrogen by a heating electrical circuit in the atomic oscillator. This purifier has been replaced by a design made from a thin nickel tube, which performs the same function but shows a more stable performance [14].

2.2.2 Preparation of H atoms

To obtain hydrogen atoms, the purified hydrogen flow leads into a dissociator designed to discharge the hydrogen molecules. An RF dissociator design is the best choice for the H-maser [10, 15] due to the simplicity in building and operating, as well as the easy ability to focus the atoms. The molecular hydrogen is then dissociated by the collisions with energetic electrons to produce atoms and more electrons and ions. Those atoms pass through a collimator made of single or multiple channels (Figure 5 [16]) and formed into an atomic beam. The atomic hydrogen beam then passes through a fractional population inversion component called the magnetic state selector, which utilizes a gradient magnetic field to deflect undesired H atoms of the level ($F = 1$, $m_F = -1$, and $F = 0$, $m_F = 0$). The flux of atoms entering the storage bulb is of the order of 10^{12}–10^{13}/sec [1]. However, the classical design could not separate undesired ($F = 1$, $m_F = 1$) level atoms from the ($F = 1$, $m_F = 0$) and effectively deflect them from the path of the useful atomic beam, as the effective magnetic moment of ($F = 1$, $m_F = 1$) had the same sign as that of the

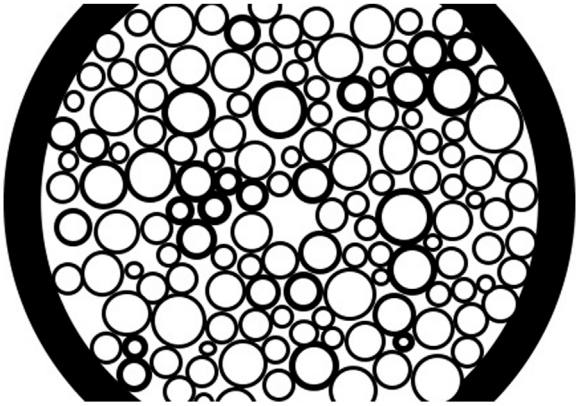

FIGURE 5
Schematic of a multichannel collimator.

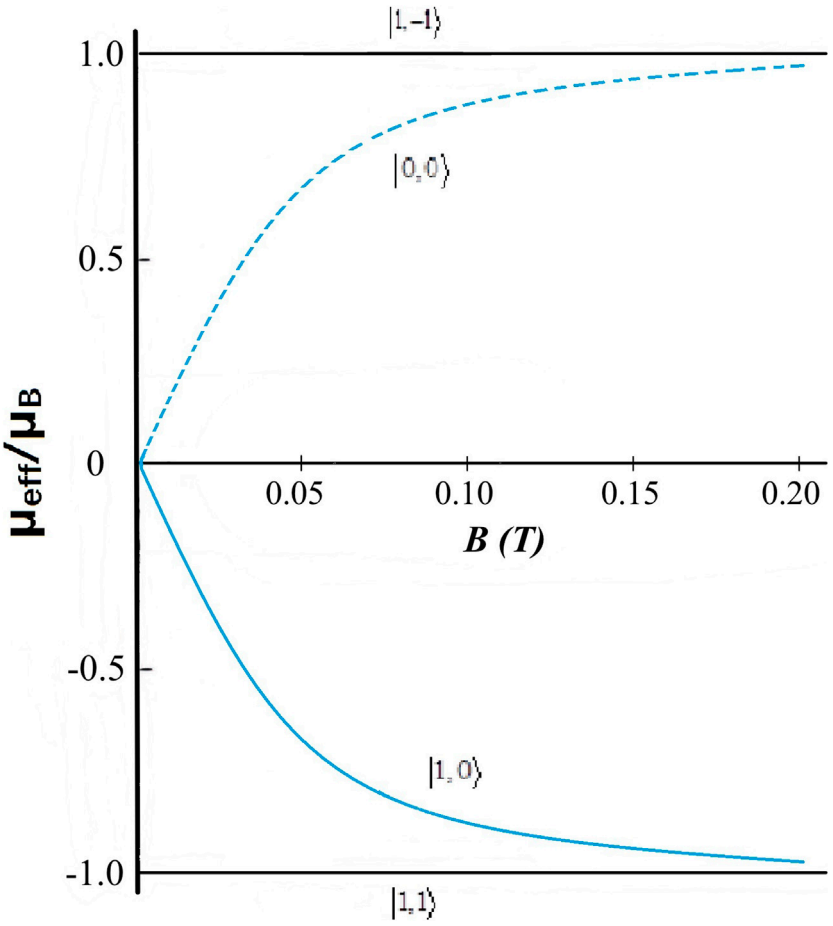

FIGURE 6
Variation of the magnetic moment with the magnetic field.

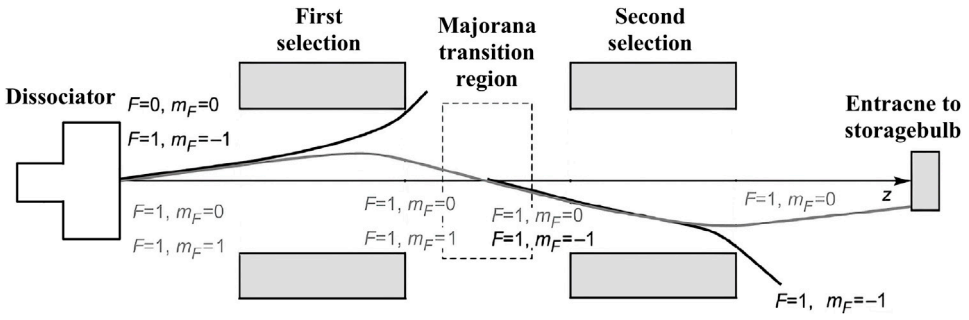

FIGURE 7
Schematic diagram of a single-state ($F = 1$, $m_F = 0$) selector for the H-maser.

($F = 1$, $m_F = 0$); thus, they underwent a deflecting force in the same direction (Figure 6). To improve the quality of the atomic transitional signal to improve the short- and long-term frequency stability performances, a single-state selection system design was proposed based on the adiabatic fast passage theory. This method was reported to remove 90%

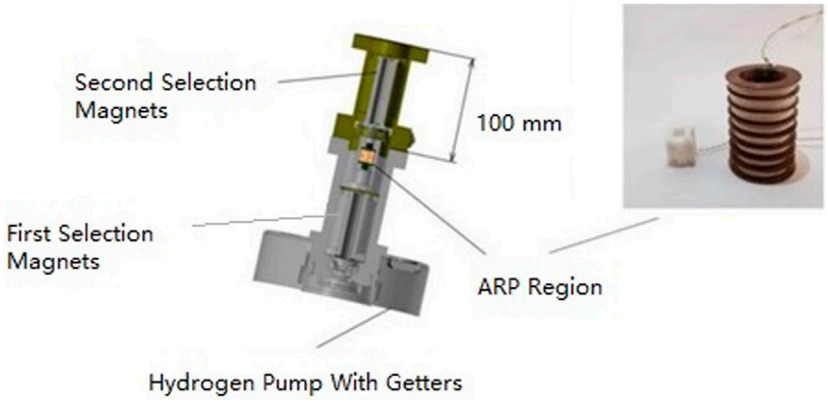

FIGURE 8
Single-state ($F = 1$, $m_F = 0$) selector using the adiabatic rapid passage (ARP) technique.

of undesired ($F = 1$, $m_F = 1$) atoms [17]. The realization of this technique in the laboratory is shown in Figure 7 [18], and Figure 8 [6]. Although the design had been proposed long ago, the technique was developed for use on commercial products for the first time. This technique contributes to the stability performance by reducing the spin exchange.

The prepared H atom ($F = 1$, $m_F = 0$) then goes into a storage bulb to undergo approximately 10^4 collisions with the wall of the bulb [1] during an average storage time of 1 s. To reduce the atomic energy perturbation, the inner surface of the bulb should carefully be coated. Long-chain paraffin and Dri-Film surfaces were attempted before Teflon was finally confirmed to be the best substance owing to its diminished chemical reaction and reduced wall shift [10].

2.2.3 Conditions for a resonant oscillation

As stated previously, the H-maser is set to a resonant oscillation. A microwave resonant cavity was designed for this purpose, based on the TE_{011} mode for the standard-sized H-maser. The electromagnetic field should have a magnetic component distribution that is symmetrically axial, with a central resonant frequency tuned to 1.420405 GHz, which is very close to the ($F = 1$, $m_F = 0$)–($F = 0$, $m_F = 0$) atomic transitions. The microwave cavity is normally made of fused silica or quartz cylinder, with its inner surface coated with silver. It is thermally regulated with a temperature variance of no more than 0.01°C, as the resonant frequency changes with temperature. The cavity can also be made of other materials such as aluminum, titanium, etc. Whatever the material, the central resonant frequency should be rigorously stabilized to a value close to the atomic transitional frequency. The quality factor, Q, should also be high enough for the resonant oscillation. A standard fused quartz cylindrical normally has unloaded and loaded Q factor values of 60,000 and around 35,000–45,000, respectively [1, 8]. The temperature coefficient is around 1 kHz/°C. Metal microwave cavities reach a higher Q factor but also a higher temperature coefficient that is often of a higher order. A higher Q factor can contribute to the coupled power; however, a higher temperature coefficient leads to difficulty in the thermal regulation of servo circuits for the cavity pulling effect. The signal of the physical unit is detected by a loop mounted on one end plate of the microwave cavity, where the magnetic field has a maximum value. The microwave cavity can be coarsely tuned by mechanical adjustment, temperature-adjusted for intermediary tuning, and finely tuned by varying the electric current of the varactor circuit.

To provide numerous atomic transitions, an approximately uniform quantization magnetic field of the order of 10^{-7} T [1] is generated by a solenoid designed to sit outside of the microwave resonant cavity and inside of the ambient magnetic field shielding layers made from a high-permeability permalloy material.

Finally, the vacuum design is generally implemented by application of the VacIon pump, with which a pressure of 10^{-5} mmHg can be maintained for a flux average of 10^{17} atoms flowing out of the collimator. Currently, the getters, as shown in Figure 8, are widely used for their ultra-high vacuum design and working stability.

2.2.4 Small H-masers

To realize and generalize the satellite on-board applications of H-masers, studies have focused on reducing the volume and mass of standard-sized H-masers. Since the volume is mainly limited by the size of the microwave resonant cavity, designs such

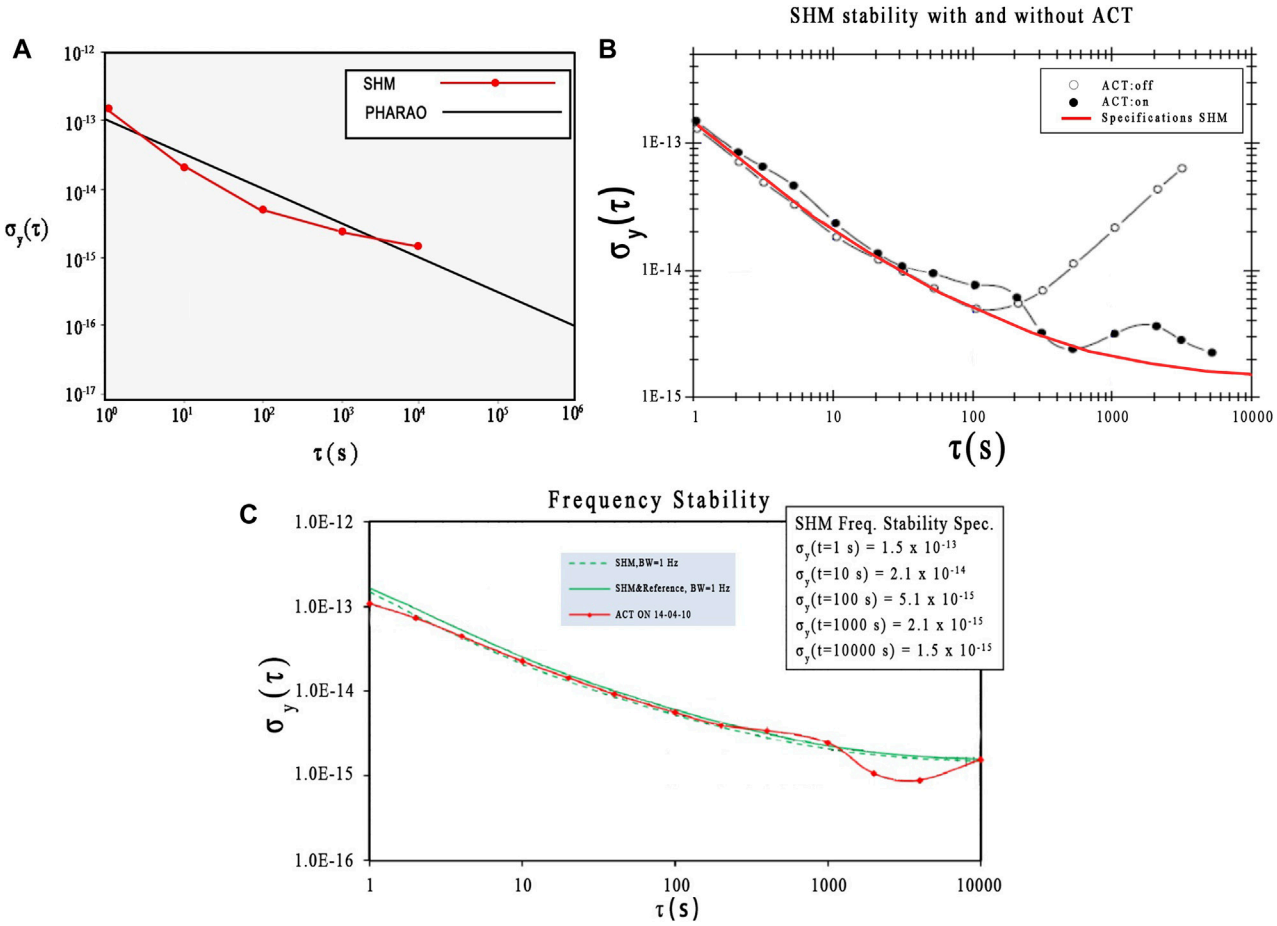

FIGURE 9
Development of the small active H-MASER (SHM). **(A)** is the stability performance of 35 kg SHM for ACES. **(B)** is comparison of the stability with the ACT on and off. **(C)** is the stabilty performance of a 40 kg SHM by SpectraTime.

as the small size TE_{111} mode microwave resonant cavity, Q-enhanced microwave cavity, and sapphire microwave resonant cavity, etc., were made for the small active H-maser.

The passive H-maser [19] has a dramatically reduced volume and mass weight by sacrificing the frequency stability performance. The physical unit techniques of passive H-maser are mostly like those of the standard-size active H-maser.

The H-maser techniques were developed to meet the demands of space experiments, including better stability performance, robustness, and environmental suitability. For on-board applications, the requirements include a smaller, lighter, and lower power consumption design. A traditional standard-sized active H-maser device is >200 kg. Improvements have led to lighter masers that are more favorable for space missions. For example, a small active H-maser (SHM) for the Atomic Clock Ensemble in Space (ACES) mission weighed only 35 kg using a sapphire microwave cavity, in the Neuchâtel observatory [20] in 2003. The frequency stability performance was 1.5×10^{-15}/10,000 s (Figures 9A,B).

The ACES utilized an SHM for its medium stability performance, together with the long-term stability performance of a cold cesium atomic clock to provide excellent stability performance [21]. The SHM by SpectraTime, weighing 40 kg, reached a stability performance of 2.1×10^{-15} (Figure 9C).

The 60 kg on-board standard active H-maser design of the sitall microwave cavity [22] from Vremya-CH of Russia was planned to be applied to the international space VLBI network (RadioAstron) for researching dark matter, redshift, etc. Its frequency stability successfully reached 2.5×10^{-15}/1,000 s (Figures 10A,B). One was launched in 2011 [23].

The Millimetron mission of the International Space Observatory proposed an updated stability performance of the

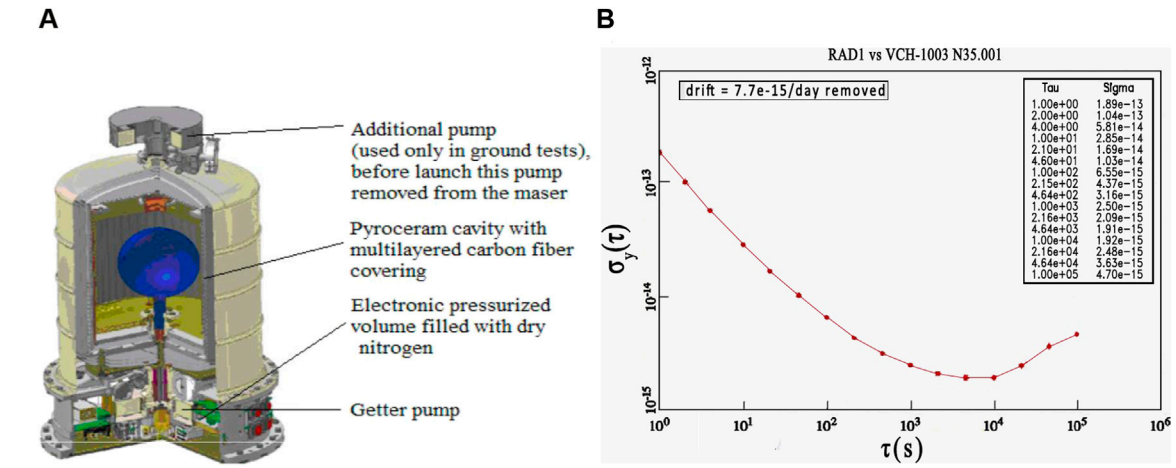

FIGURE 10
The 60 kg on-board standard active H-MASER. **(A)** the practical design. **(B)** the stability performance.

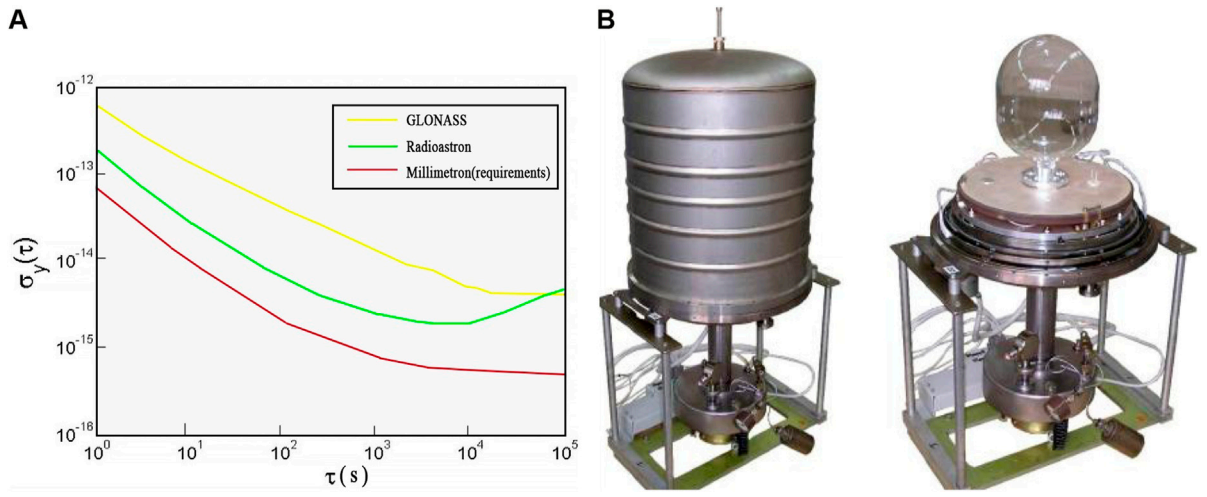

FIGURE 11
Single-state atomic beam selection standard active maser **(A)** the Millimetron requirements. **(B)** Practical design.

frequency source [22] (Figure 11A). Vremya-CH adopted a single-state atomic beam selection standard active H-maser design to meet this (Figure 11B). The microwave resonant cavity was made of titanium, likely to address the need for both toughness and high Q factor.

The advantage of passive H-maser is its small size for on-board applications. This review will not focus on this technology as the physical unit is similar in structure to that of active H-masers. The difference lies in the following. First, its smaller metallic cylindrical cavity, also in the TE_{011} mode, is made of aluminum to provide a loaded quality factor, Q_{loaded}, of no less than 5,000. Electrodes inside the cavity are designed to regulate the electromagnetic field distribution to ensure that the magnetic field is in the same direction in the enclosed space. The atomic storage bulb was also designed in the shape of a long tube according to electromagnetic field distribution. A typical design adopts three or four magnetic shielding layers to reduce the influence of ambient magnetic fields. The selector preferentially uses a quadrupole design to minimize the volume. Since it is smaller than the standard active maser, cavity thermal control is easier to accomplish. Moreover, the

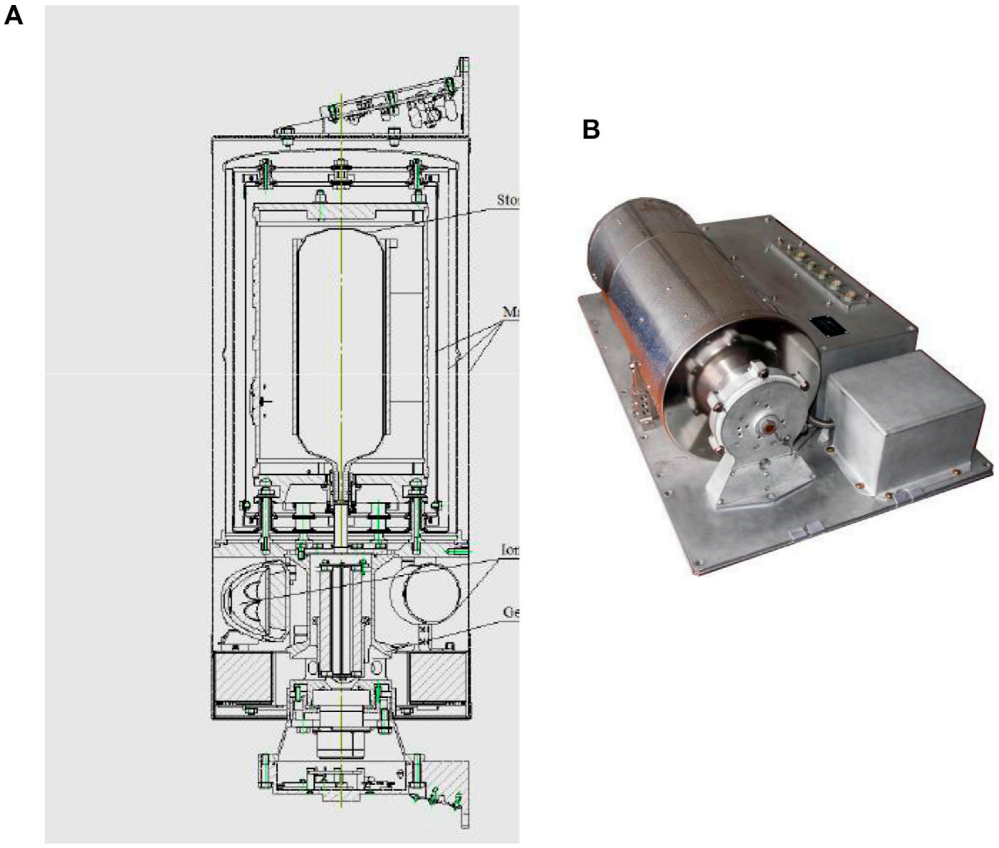

FIGURE 12
Passive H-masers. **(A)** Flight model unit designed by Vremya–CH. **(B)** Flight model passive H-maser fromVremya–CH.

mass of the hydrogen source can be optimized since the consumption is smaller. The design of the on-board passive H-maser by Vremya-CH is shown in Figure 12A [22] as an example of a satellite-based passive H-maser.

Although the stability performance is not good as that of the standard-size active H-maser, passive H-maser has been developed and widely used for GNSS. The on-board Passive H-MASER of Vremya-CH [22], shown in Figure 12B, for the GLONASS-κ had reached a stability performance of 10^{-15}/10,000 s. A Space Mini Passive Hydrogen MASER (mPHM), was carried out in the frame of the ESA European GNSS Evolutions Programme. The design possibly has reduced the mass to only 12 kg, published in 2011 [24].

In China, the stability performance of the ground-based active H-maser has reached a few parts in 10^{15} for an average interval on the order of 10^4 s, while the passive H-maser has reached a few parts in 10^{14} for 10^4 s. Meanwhile, the Beijing Institute of Radio Metrology and Measurement (BIRMM) is working on a 40 kg on-board active H-maser for the China Space Station. The Shanghai Astronomical Observatory (SHAO) has recently participated in this research and is now working on principle model research based on the standard ground-based H-maser.

3 Applications in space scientific research

3.1 The theory of relativity

H-masers can provide standard frequency signals for space experiments, in which their accuracy and stability play important roles. For example, in 1976, the H-maser was used in the famous gravitational redshift test, gravity probe A (GP-A) [25], in which the H-maser was nearly vertically shot into space at an altitude of 10,000 km on board a 100 kg spacecraft.

The experiment was carried out by NASA jointly with the Smithsonian Astrophysical Observatory (SAO). The gravitational redshift was measured by the CW microwave signal frequency comparing technique and a three-way linked Doppler canceling system. The microwave signals were respectively provided by the ground and on-board H-masers.

Allan Variance

τ	Primary Standard	Secondary Standard
1 second	1×10^{-12}	1×10^{-11}
10^4 second	1×10^{-14}	3×10^{-13}
12 hours	1×10^{-14}	3×10^{-13}
10 days	1×10^{-13}	3×10^{-13}

Power Spectral Density of Phase: BW = 1 Hz ± 10 Hz

Reference Distribution Frequency	Primary Standard	Secondary Standard
5 MHz	Better than -116 dB	Better than -110 dB
10 MHz	Better than -110 dB	Better than -104 dB
50 MHz	Better than -96 dB	Better than -90 dB
100 MHz	Better than -90 dB	Better than -84 dB

FIGURE 13
Frequency standard requirements, 1981–1986.

The relative frequency variance was determined according to the theory of relativity. The data fit Einstein's theory within the order of 10^{-6}. The precision of the experimental data was due to the (τ = 100 s) frequency stability performance of the H-masers.

3.2 The DSN and spacecraft tracking

H-masers have also been applied to the DSN for stable time and frequency reference signals [26]. Figure 13 shows the requirements proposed by the frequency and time subsystems of DSN applications, from 1981 to 1986. To synchronize the stations distributed in Spain, the United States, and Australia, a low H-maser frequency drift is desired.

In 1968, the H-maser was first put into use for the DSN; since that time, studies have been performed to assess the performance and the possibility of improvements in frequency stability. Figure 14A shows the stability performance measurement of an H-maser with environmental temperatures varying within 0.05°C. The curve starts to go up when τ is approximately 10^3 s. As environment effects and maser aging were attributed to these observations, relevant improvements have been proposed.

Meanwhile, the spacecraft tracking and detecting technique has been used for analyses of planet atmospheres, navigation, distance ranging, and gravitation detection. Observations including the phase, retardation, and amplitude of the transmitted signals can be acquired from the radio waves either sent from the spacecraft and received by a ground station or sent by a station on the ground, transponded by a spacecraft, and received by another ground station. One-, two-, and three-way modes have been established for deep space tracking. Synchronization between stations and antennas is important for the accuracy of tracking and precision of experiments. The H-maser frequency stability performance for deep space tracking in 1991, shown in Figure 14B [27], reached 10^{-16} for $\tau = 10^3$ s. The proposed requirement for the H-maser in the Cassini gravity wave experiment in 1998 was even lower part in 10^{16}.

3.3 The VLBI network

The H-maser is widely used in the very long baseline interferometry network. In the early Orbiting VLBI mission of RadioAstron, the CRONOS experiment [28] was postponed and eventually aborted due to funding challenges [29] but was proposed for space radio telescope receiving, space VLBI observation, Global Satellite Navigation, and gravitational wave detection. An active H-maser system was planned for both ground stations and spacecraft. A sapphire-design microwave cavity small H-maser (SHM), for on-board spacecraft use was developed in 1999 and weighs only 50 kg [30].

Given the technical advantages and high-resolution observations in the VLBI, this system has been used for research on black holes. In the international Earth Horizon Telescope (EHT) project, a huge telescope with a size equivalent to that of the Earth is approximated by relevant worldwide distributed individual telescopes. The quality of the

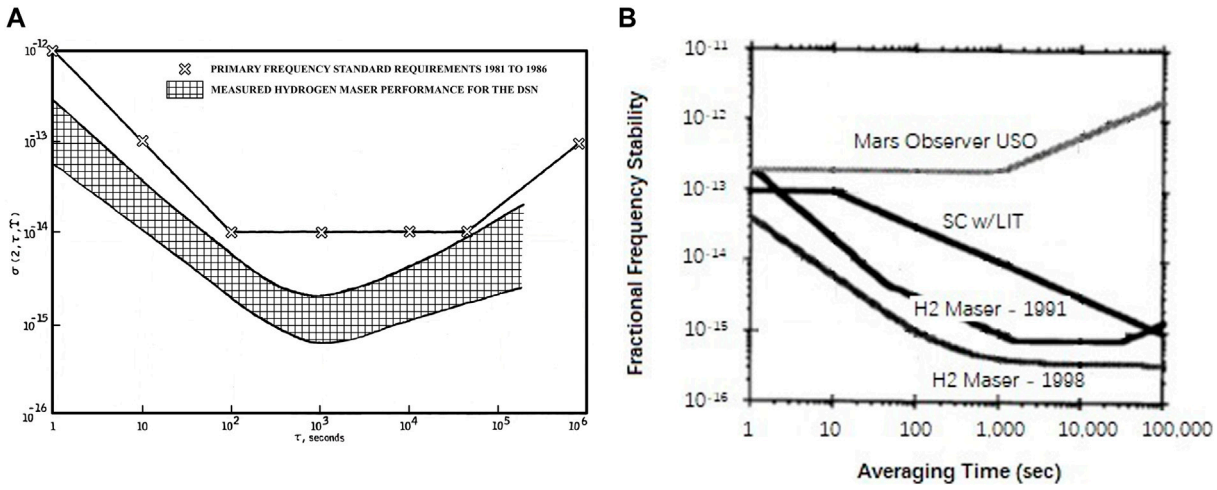

FIGURE 14
Frequency stability performace of the H-Masers for the deep space network (DSN) **(A)** measured stability with the envirionmental temperature varying no more than 0.05°C. **(B)** stability performance for deep tracking in 1990s.

black hole imaging depends on the resolution of the observations, as well as the precise synchronization between individual telescopes, to which the high stability performance of active H-maser units has contributed.

The H-maser has also contributed to the international Square Kilometre Array Telescope (SKA), which is researching on the origin of the universe, space magnetic field distribution, etc., and to the Millimetron projects for even higher sensitivity, millimeter and submillimeter resolution, and infrared observation.

3.4 The GNSS

H-masers are currently widely used in the Global Navigation Satellite System, including GPS in the United States, GLONASS in Russia, GALILEO in Europe, and BDS in China. Besides the high-quality ground-based active H-maser for the ground station, high-quality satellite-based passive H-maser also plays role in the system and promotes the precision of information on the position, time, and speed in space. A typical design adopts one or two on-board passive H-maser systems as the satellite standard frequency source.

4 Discussion

4.1 Summary of recent technique developments

The H-maser is currently widely used worldwide. The research institutions and their latest updates are the following.

The active H-maser MHM-2020 from the Microsemi company in the United States has reached a stability performance of 2.0×10^{-15} (τ = 1,000 s). The VCH-1003M from Vremya-CH in Russia also features a stability of 2.0×10^{-15} for its commercial product. However, the single-state selection beam system design has reached a stability of 6.69×10^{-16} (τ = 1,000 s) and better than 1×10^{-16} (τ = 100,000 s). The iMaser 3000 from T4 Science in Switzerland has reported a stability of 8.71×10^{-16} (τ = 1,000 s). In China, the BIRMM and SHAO have reported H-maser stability values of approximately 5×10^{-15} (τ = 1,000 s).

Among passive H-maser devices, the VCH-1008 from Vremya-CH has reached a stability of 4×10^{-15} (τ = 1 day). The pH Maser 1008 from T4 Science has a stability of 4×10^{-15} (τ = 1 day) too. The passive H-MASER of BIRMM and SHAO have reached the order of 10^{-15} (τ = 1 day).

Concerning the requirements for small size and low mass in the context of space experiments, recent studies have focused on smaller microwave resonant cavities. A smaller cavity constructed of a material with a higher dielectric constant; for example, sapphire has been designed for on-board applications. Metallic cavities of aluminum or titanium have also been developed to improve the robustness and quality factor of the H-maser device. However, their temperature coefficients are higher than those for standard fused quartz cavities, which may negatively affect the stability performance of the H-maser.

Second, pump development has improved the background vacuum of the H-maser. These advances have solved the requirements for lower mass and better vacuum performance and are currently widely used in on-board applications.

Third, the single-state selection beam system has recently improved the stability of the H-maser to better than $1 \times 10^{-16}/10^5$ s, although the realization of this technique is complicated.

4.2 Improvements

H-masers still have space for improvement. Future technique developments will aim to improve the stability performance and miniaturization for space science research.

First, as the stability performance is sensitive to the thermal noise of the microwave cavity and the first-stage receiver, cooling may be one direction for improvement. Atomic oscillation signals were observed by Vessot et al. at the Smithsonian Observatory in studies using a cold h-maser [31]. The estimated average stability performance was 10^{-18} for 10^3s. This solution may warrant efforts toward manufacturing.

Secondly, among room-temperature standard H-masers, the frequency shift mainly occurs due to the second-order Zeeman frequency shift $\Delta\omega_z$, wall shift $\Delta\omega_W$, spin exchange shift $\Delta\omega_e$, and shift induced by the atomic motion in a non-homogeneous magnetic field $\Delta\omega_m$, in terms of the H-maser principles [1, 2], as expressed in Formula 9:

$$\boldsymbol{\omega_0 = \omega_H + \Delta\omega_z + \Delta\omega_W + \Delta\omega_e + \Delta\omega_m} \quad (9)$$

Thus, the performance of the magnetic shielding layers, as well as the wall coating and vacuum techniques, can be improved to reduce the relevant frequency shifts.

Improvements can also result from material science research. For example, the development of ambient magnetic field shielding techniques involves improved permeability, which may include research on the alloy constitution and heat-treating techniques. These advances should contribute to the stability performance of the H-maser by increasing the magnetic shielding efficiency. Another potential example is research on the wall shift, which requires a deeper understanding of the interaction between hydrogen atoms and the coated Teflon layers.

Finally, the failure modes of H-masers have been studied [32]. The dissociator of the maser is used to generate ground atomic hydrogen; although it was developed long ago, we still have not fully solved the problem of efficiently generating atoms due to the complexity of the reaction inside the plasma [33]. Simulations may be useful for addressing this challenge. Another question is the aging speed of the discharging bulb. The ions in plasma continuously collide with the wall of the bulb. Bulb aging is closely related to surface damage caused by impacts and the high temperature in plasma. The surface damage may increase the probability of recombination, which may decrease the discharging efficiency and is critical for long-term H-maser performance.

Author contributions

JD contributed predominantly to this work. All authors participated in the writing of the manuscript.

Acknowledgments

I acknowledge the contributions of Professor Yiqiu Wang to this study. Professor Yiqiu Wang has often visited our institute and has provided many forms of help. He kindly prepared a series of seminars and lectured with passion as a qualified and patient scientist. We have discussed research regarding the H plasma of the H-maser and confirmed the value of this work. He introduced me to another Professor experienced in plasma and optics when he discovered that I was applying for the NSFC and seeking a collaboration. He was invited to join my seminar talk in the summer of 2019 and provided instruction not only on issues related to the hydrogen maser but also on atomic physics. Moreover, I learned the spirit of Beijing University from him and I am also learning from him how to teach my students. He is a real educator.

Conflict of interest

The authors declare that the research was conducted in the absence of any commercial or financial relationships that could be construed as a potential conflict of interest.

Publisher's note

References

1. Vanier J, Claude A. *The quantum physics of atomic frequency standards*. Bristol and Philadelphia: Adam Hilger (2022).

2. Active Hydrogen Maser. Product directory clocks frequency references 3833 active hydrogen maser (2020). Available from: https://www.microsemi.com/product-directory/clocks-frequency-references/3833-active-hydrogen-maser Accessed July 7, 2022.

3. Frequency Standards and Frequency References. Product directory cesium frequency references (2022). Available from: https://www.microsemi.com/

product-directory/cesium-frequency-references/4115-5071a-cesium-primary-frequency-standard#resources Accessed July 9, 2022.

4. Standard Research Systems. Rubidium frequency std (2022). Available from: https://www.thinksrs.com/products/fs725.html Accessed July 15, 2022.

5. Kleppner D, Goldenberg H, Ramsey NF. Theory of the hydrogen maser. *Phys Rev* (1962) 126:603–15. doi:10.1103/physrev.126.603

6. Polyakov V, Timofeev Y, Demidov N. *Frequency stability improvement of an active hydrogen maser with a single-state selection system, page 127, 2021 China Time & Frequency Symposium*. Gansu, China: Dunhuang (2021). p. 13.

7. Time Realization And Distribution. Time and frequency from A to Z, H (2022). Available from: https://www.nist.gov/pml/time-and-frequency-division/popular-links/time-frequency-z/time-and-frequency-z-h#hydrogenmaser Accessed July 7, 2022.

8. Demidov NA. The development and futrue of hydrogen maser clock technology. *J Astronomical Metrology Meas* (2007) 6. doi:10.3969/j.issn.1000-7202.2007.z1.002

9. Ramsey NF. The atomic hydrogen maser. *Metrologia* (1965) Vol. 1:5–15. doi:10.1088/0026-1394/1/1/004

10. Kleppner D, Berg HC, Crampton SB, Ramsey NF, Vessot RFC, Peters HE, et al. Hydrogen-Maser principles and techniques. *Phys Rev* (1965) 138:A972–83. doi:10.1103/physrev.138.a972

11. Vessot R, Levine M, Mueller L, Baker M. *The design of an atomic hydrogen maser system for satellite experiments, 21st annual symposium on frequency control*. Fort Monmouth,NJ,USA (1967). p. 24.

12. Active Hydrogen Maser VCH-1003M. *Active hydrogen MASER VCH-1003M operations manual, 411141.032 OM*. Nizhny Novgorod: VREMYA-CH" JS Company (2006).

13. Dai J, Lin C. Hydrogen absorbing alloys application in hydrogen MASER. *Ann Shanghai Astronomical observatory, CAS, No.* (2007) 28:160.

14. Qi L, Hou X, Dai J, Chen Z, Liu T, Yang H. Research on a material for hydrogen purifying and flux controlling with application to space active hydrogen-masers. *AIP Adv* (2022) 12:035207. doi:10.1063/5.0084176

15. Maleki L. A study of the processes in the RF hydrogen gas dissociator. *TDA Prog Rep* (1980):42.

16. Vessot RFC, Peters HE. *Design and performance of an atomic hydrogen maser*, 183. Ire Transactions On Instrumentation. doi:10.1109/IRE-I.1962.5006627 (1962).

17. Mattison EM, Vessot RFC. Single state selection system for hydrogen masers. In: Proceedings of the Nineteenth Annual Precise Time and Time Interval (PTTI) Applications and Planning Meeting. Redondo Beach, CA (1987). p. 1.

18. Belyaev AA, Demidov NA, Polyakov VA, Timofeev YV. Estimation of the possible reduction of the limit frequency instability of A hydrogen generator using an atom beam in one quantum state. *Meas Tech* (2018) 61:779–83. doi:10.1007/s11018-018-1501-7

19. Howe DA, Walls FL, Bell HE, hellwig H, Small A. *Passively operated hydrogen maser, 33rd annual symposium on frequency control*. Atlantic City, NJ, USA (1979).

20. Jornod A, Goujon D, Gritti D, Bernier LG. The 35kg space active hydrogen maser (SHM-35) for ACES. In: Proceedings of the 2003 IEEE International Frequency Control Symposium and PDA Exhibition Jointly with the 17th European Frequency and Time Forum (2003).

21. Goujon D, Rochat P, Mosset P, Boving D, Perri A, Rochat J, et al. *Development of the space active hydrogen maser for the ACES mission, EFTF-2010 24th European frequency and time forum*.

22. Belyaev AA, Demidov NA, Medvedev SY, Pavienko YK, Sakharov BA, Vorontsov VG. Russian hydrogen masers for ground and space applications, 2019 URSI Asia-pacific radio science conference (AP-RASC), March 2019. doi:10.23919/URSIAP-RASC.2019.8738340 (2015).

23. Belyaev AA, Demidov NA, Gorelov SD, Polyakov VA, Sakharov BA, SkrylTimofeev ASYV. *On-board active hydrogen maser for Millimetron project, China satellite navigation conference*. China: Harbin (2018).

24. Belloni M, Gioia M, Mosset P, Waller P, Busca G. Space Mini passive hydrogen maser- A compact passive hydrogen maser for space applications. In: IEEE 2011 Joint Conference of the IEEE International Frequency Contral and the European Frequcny and Time Forum (FCS). San Francisco, CA, USA (5201). doi:10.1109/FCS.2011.5977320

25. Vessot RFC, Levine MW, Mattison EM, Blomberg EL, Hoffman TE, Nystron GU, et al. Test of relativistic gravitation with a space-borne hydrogen maser. *Phys Rev Lett* (1980) 45:2081–4. doi:10.1103/physrevlett.45.2081

26. Kuhnle PF, Sydnor RL. Present and future frequency and timing capabilities of the deep space network. *J Phys Colloques* (1981) 42:C8-373–81c8381. doi:10.1051/jphyscol:1981844

27. Border JS, Robert Kursinski E. *Deep space tracking and frequency standards*, Los Angeles, CA: Forty-Fifth Annyal Symposium On Frequency Control, IEEE. doi:10.1109/FREQ.1991.145957 (1991).

28. Busca G, Bernier LG, Schweda H, Kardashev N, Andreianov V, Toxburgh IW, et al. The cronos hydrogen maser clock redshift experiment on Radioastron. *Adv Space Res* (2003) 32(7):1421–8. doi:10.1016/s0273-1177(03)90356-5

29. Schweda H, Zivanov S, Perruchoud G, Weber C, Thieme B, Baister G. Performance demonstration of the on-board active hydrogen maser for the ACES space mission of ESA. In: 2007 IEEE International Frequency Control Symposium Joint with the 21st European Frequency and Time Forum.

30. Bernier LG, Jornod A, Schweda H, Gentsch R, Busca G. *The SHM hydrogen atomic clock for space applications: Development and test of the PEM physics package, 29th annual precise time and time interval*. California: PTTI Meeting (1997). p. 61–8.

31. Vessot RFC, Mattison EM, Imbier E. Cold hydrogen maser research at SAO and related developments. In: IEEE 37th Annual Symposium on Frequency Control (1982).

32. Popa AE, Wang HTM, Bridge WB, Chester AN, Etter JE, Walsh BL. A study to identify hydrogen maser failure modes. In: Hughes Research Laboratories, 30th Annual Symposium on Frequency Control (1976).

33. van Schreven E, Belloni M. *Hydrogen plasma simulation for atomic clock lifetime assessment*. York, United Kingdom: IEEE 2016 European Frequency and Time Forum (EFTF). doi:10.1109/eftf.2016.7477811 (2016).